International Journal of Research
Available at https://edupediapublications.org/journals
e-ISSN: 2348-6848
p-ISSN: 2348-795X
Volume 05 Issue 04
February 2018

Design and Analysis of Modular Multilevel Cascaded Converter (Mmcc-Ssbc) Based Fuzzy Controller with Battery Energy Storage System

Balla Satya Durga Prasad & B Baby
[1]M.Tech(Student), Kakinada Institute of Technological Sciences Affiliated to JNTUK, KAKINADA, Andhra Pradesh, India
[2]Assistant Professor, Kakinada Institute of Technological Sciences Affiliated to JNTUK ,KAKINADA, Andhra Pradesh, India.

ABSTRACT- *An enhancement of performance and availability of battery energy storage system using a modular multilevel cascaded converter based on fuzzy controller has to be implemented in this paper for flexibility control. Here we are using the fuzzy logic controller, because it has many advantages comparing to other controllers. Such as, the fuzzy controller is the most suitable for the human decision-making mechanism, providing the operation of an electronic system with decisions of experts. The SSBC-based BESS produces three-phase multilevel voltage waveforms, and eliminates both harmonic filters and a complicated zig-zag transformer from the ac side. The circuit control modularity of the SSBC enables the usage of multiple individual low-voltage battery modules. Along with control strategy based on zero-sequence-voltage injection, this modularity enhances the availability and flexibility of the BESS by using fuzzy controller. The BESS with fuzzy provides low harmonic distortion compared to traditional system even when it operates with different active-power commands for individual bridge cells. In addition, zero-voltage ride-through (ZVRT) capability is verified for the severest single-phase, two-phase and three-phase voltage sags. Mathematical analysis and simulation verification validate the downscaled system and performance, making the BESS prospective.*

Index Terms—Battery energy storage systems (BESSs), cascade connections, modular multilevel cascade converters (MMCC), phase-shifted-carrier pulse-width modulation (PWM), zero-voltage-ride-through (ZVRT) capability, Fuzzy controller.

INTRODUCTION

The past decade, renewable energy sources such as photovoltaics and wind-power generation have been progressively installed within distribution power systems. However, the output power of photovoltaics and wind-power generation depends significantly on weather and climate conditions. Electric power utilities may face system stability issues related to voltage and frequency fluctuations resulting from the intermittent nature of renewable energy sources. A battery energy storage system (BESS) has the capability of releasing active power to, or absorbing it from, its installation point to mitigate such voltage and frequency fluctuations in a distribution power system. This justifies the installation of the BESS on the distribution system, to support massive installation of renewable energy sources.

An early BESS intended for distribution power systems was based on the combination of 18-, 24-, 36-, or 48-pulse converters with a three-phase zig-zag transformer. The use of multiple complicated phase-shifted windings brings various difficulties to the design and construction of the zigzag transformer, thus resulting in raising an issue of insulation reliability.

The parallel connection of multiple battery strings, each of which is based on series-connected battery modules, results in higher dc voltages and higher power ratings. However, increasing the number of the series-connected battery modules brings complexity to the battery management system. Moreover, even when only a single battery module in a battery string fails, the corresponding string should be disconnected. Such a situation either reduces the power rating drastically or forces the shutdown of the BESS for safety reasons.

Some research papers have discussed SSBC-based BESS configurations including simulated results in this paper. The SSBC-based BESS is characterized by allowing a low voltage battery string to be installed on the dc side of each bridge cell, because the dc voltage can be reduced. As a result, the overall failure rate of the BESS is actually reduced because the SSBC-based BESS can continue operating seamlessly even when a battery string becomes unhealthy or faulty. The SSBC-based BESS is characterized by allowing a low voltage battery string to be installed on the dc side of each bridge cell, because the dc voltage can be reduced. It clarifies the advantages of the modularity of the bridge cells in consideration of the design of an SSBC-based BESS. In addition, this paper verifies the zero-voltage ride-through (ZVRT) capability, which has not been resented by any technical paper.

The BESS can maintain seamless operation even for the most severe voltage-sag conditions, thus verifying high availability and flexibility. Experimental results show the applicability of the SSBC-based BESS to utility power distribution networks.

THE BATTERY ENERGY STORAGE SYSTEM BASED ON SINGLE-STAR BRIDGE-CELLS

Modularity and Availability

Fig. 1(a) shows the circuit configuration for a conventional BESS combining a central converter with multiple battery strings connected in parallel. A commercial BESS employs a two- or three-level neutral-point clamped (NPC) converter as the central converter. The parallel connection showed in Fig. 1(a) is required for the battery strings, each of which consists of series-connected battery modules.

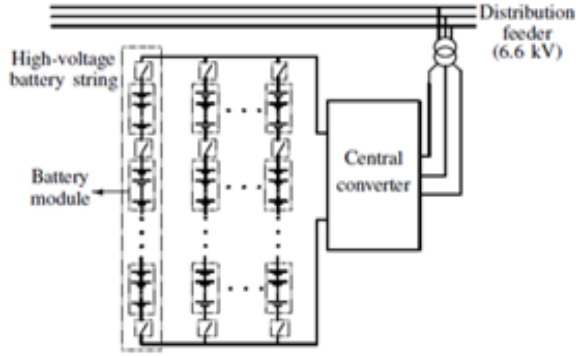

(a) The use of a single central converter with several parallel-connected high-voltage battery strings.

Fig. 1(b) shows the circuit configuration of an SSBC-based BESS. Battery strings, each of which consists of a low-voltage battery module, are connected individually to each SSBC bridge cell. Since the dc voltage of each bridge cell is reduced when compared to that of the central converter shown in Fig. 1(a), it is possible to apply a low-voltage battery string on each bridge cell.

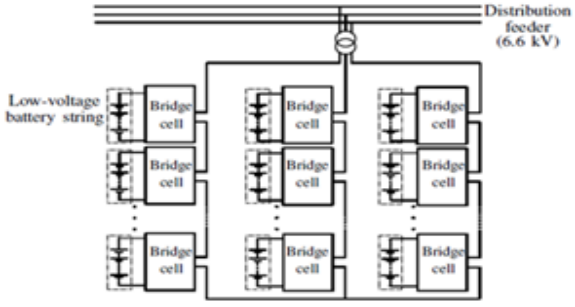

(b) The use of an SSBC with multiple floating, isolated low-voltage battery strings.

Fig. 1. Two possible BESS configurations.

Low-Voltage and Zero-Voltage Ride-Through Capability

An actual SSBC-based BESS would be intended for installation either at the secondary side of a primary distribution transformer or in the vicinity of distributed renewable energy sources within a distribution feeder. In this case, voltage sags often occur on distribution feeders as a result of line faults that happen upstream of the primary side of the primary distribution transformer.

CIRCUIT CONFIGURATION OF THE SIMULATED SSBC-BASED BESS

Main Circuit Configuration of the Three-Phase BESS Rated at 140 V, 10 kW and 21 kWh

Fig. 2 shows the power circuit configuration of the SSBC based BESS equipped with 18 lithium-ion (Li-ion) battery modules.

The SSBC-based BESS consists of three clusters with star configuration through the common point M. Each cluster consists of the cascade connection of six full-bridge or H bridge cells, and the SSBC is connected to the ac mains through an ac inductor per phase.

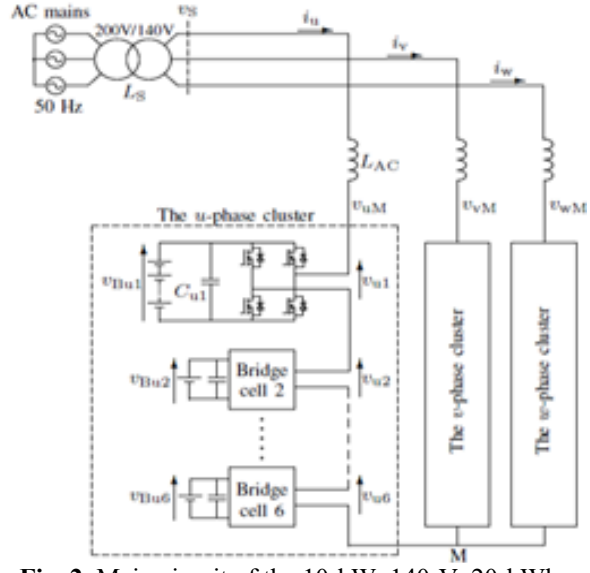

Fig. 2. Main circuit of the 10-kW, 140-V, 20-kWh SSBC-based BESS.

TABLE I
CIRCUIT CONSTANTS AND CONTROL PARAMETERS IN FIG. 2

Nominal line-to- line rms voltage	V_s	140V
Rated converter capacity		10kW
Rated energy capacity		21kWh(22MJ)
Cascade count per cluster	N	6
Background system inductance	L_s	0.10mH (1.6%)
AC inductance	L_{AC}	0.33Mh (5.3%)
Nominal battery voltage	V_B	25.9V
DC capacitance	C	47mF
Unit capacitance constant	H	29ms at 25.9V
PWM carrier frequency	f_c	1.75kHz
Equivalent PWM carrier frequency		21 kHz
Dead time		4μs

Tables I and II summarize the circuit and control parameters of the BESS and the electric specifications of each Li-ion battery module respectively. Note that the battery current contains a dc component and a 100-Hz ac component.

TABLE II
SPECIFICATION OF AN INDIVIDUAL BATTERY MODULE

Nominal terminal voltage	25.9V(7*3.7V/battery cell)
Operating voltage range	19.3-28.2V
Rated power capacity	1.2kwh(47.5Ah)

CONTROL SYSTEM

Fig. 3 shows the control and data-acquisition systems of the SSBC-based BESS. The three-phase ac mains line-to-line voltages and line currents can be detected through voltage and current sensors, respectively, and are converted to digital signals by A/D converters. The terminal voltages v_{Bu1}, v_{Bu2}…, and v_{Bw6} of the 18 battery modules are detected through 18 voltage sensors installed on the dc capacitors of all the bridge cells.

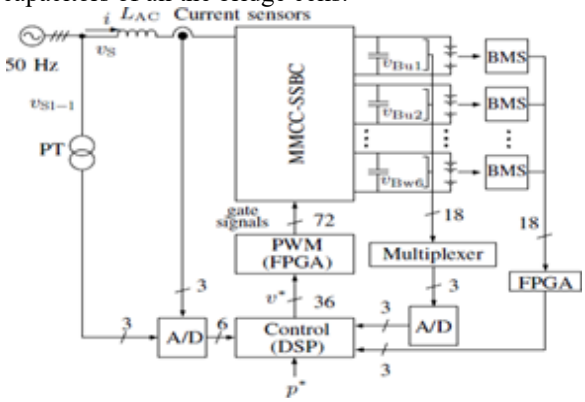

Fig. 3. Control and data-acquisition systems of the SSBC-based BESS.

Phase-shifted-carrier PWM is adopted to synthesize the multilevel voltage waveforms of the SSBC-based BESS. The implementation of the control system is simple even when the cascade count gets higher (e.g., N = 10). The constant switching frequency results in equal power losses on every bridge cell, thus leading to a simple design of heat sinks and cooling equipment for the bridge cells.

ACTIVE-POWER CONTROL OF INDIVIDUAL BRIDGE CELLS BASED ON POWER ESTIMATION

Operating Principles

The main idea is to inject a zero-sequence voltage reference v_0 into each cluster reference voltage.

The reference of the zero-sequence voltage is defined by

$$v_0^* = \sqrt{2}V_0 \sin(\omega t + \emptyset_0) \quad (1)$$

$$\emptyset_0 = tan^{-1}\left(\frac{i_q}{i_d}\right) + tan^{-1}\left(\frac{2}{\sqrt{3}}\left(\frac{1}{2} + \frac{\Delta P_v}{\Delta P_u}\right)\right) \quad (2)$$

$$V_0 = \frac{\Delta P_u}{I\cos(\emptyset_0)} \quad (3)$$

Although v_0 is added as a feed forward term, the active power feedback loop is implemented to assure the power matching between the ac and the dc sides of each bridge cell.

Battery-Current estimation

It is characterized by combining the cluster current flowing at the ac side of the BESS (see Fig. 3) with PWM switching states. Although this method resembles existing techniques for estimating the average power of each chopper-cell in the so-called "MMCC-DSCC" (modular multilevel cascaded converter based on double-star chopper cells).

Fig. 4 show four possible switching patterns for a bridge cell in the u-phase cluster. When the pattern shown in Fig. 4 (a) occurs, i_B and i_u are the same. When the pattern in (b) occurs, i_B has the inverse value of i_u.

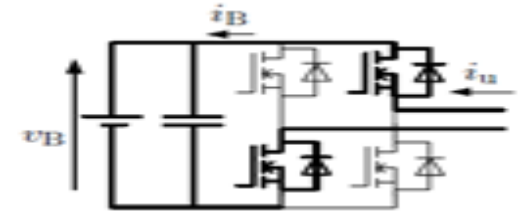

(a)

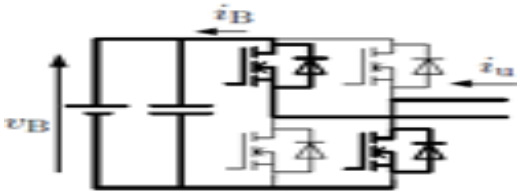

(b)

In case of either pattern shown in (c) or (d), i_B is zero. Considering the four switching patterns, the switching function SW(t) can be defined as follow;

$$SW(t) = \begin{cases} 1\ for\ the\ pattern\ in(a) \\ -1\ for\ the\ pattern\ in\ (b); \\ 0\ for\ the\ patterns\ in\ (c) and\ (d) \end{cases} \quad (4)$$

From the switching function SW(t) and the u-phase cluster current i_u, the battery current i_B can be obtained by

$$i_B = SW(t) * i_u \quad (5)$$

As an alternative to (5), the following equation exists.

$$i_B = mi_u \quad (6)$$

where m is a modulation index of the bridge cell. The value of m is given as a ratio of the ac-voltage reference of the bridge cell with respect to the corresponding dc capacitor voltage.

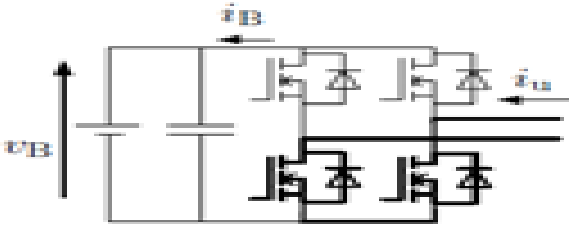

(c)

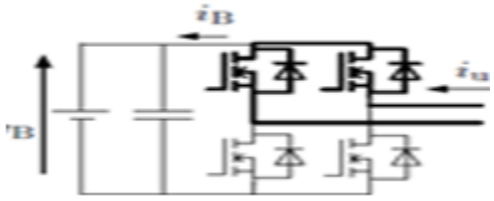

(d)

Fig. 4. Four possible switching patterns during the operation of a bridge cell. **(a)** When $i_B = i_u$. **(b)** When $i_B = -i_u$. **(c)** and **(d)** When $i_B = 0$.

The authors prefer (6) to (5) because the signal process for acquiring the switching patterns may cause a delay time in the digital controller. Hence, the power of each bridge cell in the u-phase cluster can be estimated by

$$\hat{p} = v_B m i_u \quad (7)$$

Here, ˆp contains both a dc component and a 100-Hz ac component. To extract the dc component, a moving-average filter (MAF) is used, which is similar to the one described.

Limitations on the Bridge Cell Active Power Flow

The estimated power in (7) depends on the actual value of m, which changes with the ac-voltage reference of each bridge cell. Since no over modulation is desirable for stable operation of the SSBC-based BESS, a theoretical limit should be imposed on the power output of each bridge cell. In other words, the modulation index is limited to

$$|m| \leq 1 \quad (8)$$

$$|m| = \left|\frac{\sqrt{6}V_s\bar{P}}{V_B P}\right| \leq 1 \quad (9)$$

Here, ¯p corresponds to the dc component of the estimated power ˆp, P to the BESS rated power of 10 kW, V_B to the nominal battery module terminal voltage.

FUZZY LOGIC CONTROLLER

In FLC, basic control action is determined by a set of linguistic rules. These rules are determined by the system. Since the numerical variables are converted into linguistic variables, mathematical modeling of the system is not required in FC.

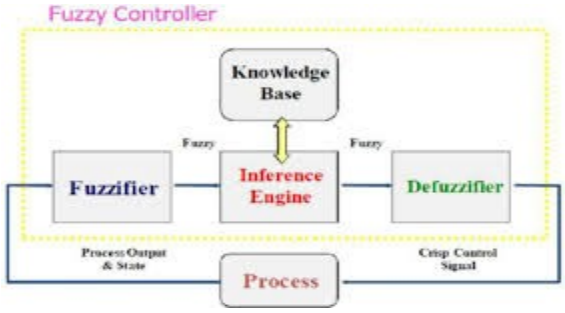

Fig.5. Fuzzy logic controller

The FLC comprises of three parts: fuzzification, interference engine and defuzzification. The FC is characterized as i. seven fuzzy sets for each input and output. ii. Triangular membership functions for simplicity. iii. Fuzzification using continuous universe of discourse. iv. Implication using Mamdani's, 'min' operator. v. Defuzzification using the height method.

TABLE III: Fuzzy Rules

e/e-	NB	NM	NS	ZE	PS	PM	PB
NB	NB	NB	NB	NB	NM	NS	ZE
NM	NB	NB	NB	NM	NS	ZE	PS
NS	NB	NB	NM	NS	ZE	PS	PM
ZE	NB	NM	NS	ZE	PS	PM	PB
PS	NM	NS	ZE	PS	PM	PB	PB
PM	NS	ZE	PS	PM	PB	PB	PB
PB	PB	PS	PM	PB	PB	PB	PB

Fuzzification: Membership function values are assigned to the linguistic variables, using seven fuzzy subsets: NB (Negative Big), NM (Negative Medium), NS (Negative Small), ZE (Zero), PS (Positive Small), PM (Positive Medium), and PB (Positive Big). The value of input error and change in error are normalized by an input scaling factor. In this system the input scaling factor has been designed such that input values are between -1 and +1. The triangular shape of the membership function of this arrangement presumes that for any particular E(k) input there is only one dominant fuzzy subset. The input error for the FLC is given as

$$E(k) = \frac{P_{ph(k)} - P_{ph(k-1)}}{V_{ph(k)} - V_{ph(k-1)}} \quad (10)$$

$$CE(k) = E(k) - E(k\text{-}1) \quad (11)$$

Inference Method: Several composition methods such as Max–Min and Max-Dot have been proposed in the literature. In this paper Min method is used. The output membership function of each rule is given by the minimum operator and maximum operator.

Defuzzification: As a plant usually requires a non-fuzzy value of control, a defuzzification stage is needed. To compute the output of the FLC, "height" method is used and the FLC output modifies the

International Journal of Research
Available at https://edupediapublications.org/journals
e-ISSN: 2348-6848
p-ISSN: 2348-795X
Volume 05 Issue 04
February 2018

control output. Further, the output of FLC controls the switch in the inverter. In UPQC, the active power, reactive power, terminal voltage of the line and capacitor voltage are required to be maintained. The set of FC rules are derived from

$$u=-[\alpha E + (1-\alpha)*C] \quad (12)$$

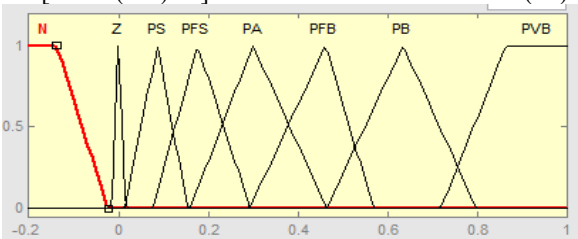

Fig.6. Input error as membership functions

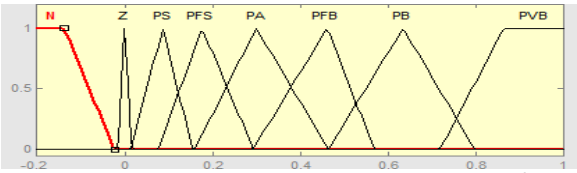

Fig.7. Change as error membership functions

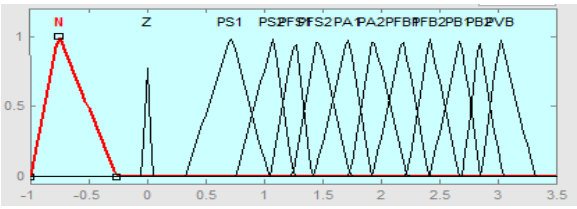

Fig.8. Output variable Membership functions

Where α is self-adjustable factor which can regulate the whole operation. E is the error of the system, C is the change in error and u is the control variable

SIMULATION VERIFICATION OF ACTIVE-POWER CONTROL FOR INDIVIDUAL BRIDGE CELLS BASED ON POWER ESTIMATION

Simulation Waveforms during Steady-State and Transient Operation

Figs. 9 and 10 show the waveforms during steady-state and transient operation when the active-power control of individual bridge cells was utilized.

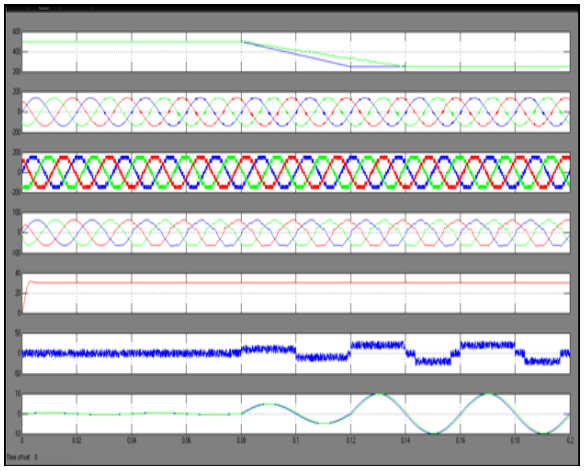

Fig. 9. Simulation waveforms for a transient response of the active-power reference of the u-phase battery module numbered 1 from 500 to 250 W when the active-power control for individual bridge cells was applied during charging operation.

Fig.9 shows those when the power reference p_{u1} was changed from 500 W to 250 W in 20 ms. Before p_{u1} was changed, all bridge cells had the same power reference as 500 W. The overall power reference p was 9 kW, and the current THD on the u-phase cluster was 2.8%.

Fig.10. shows the waveforms when p_{u1} was changed from 250 W to 0 W in 20 ms. After the transient operation, p was reduced to 8.5 kW, the three-phase currents were still balanced. The current THD on the u-phase cluster was 2.8%.

Discussion on the zero-sequence voltage and the nominal voltage of battery modules

The tested BESS can produce three-phase balanced currents even when one battery module has a null power, as shown in Fig.10.

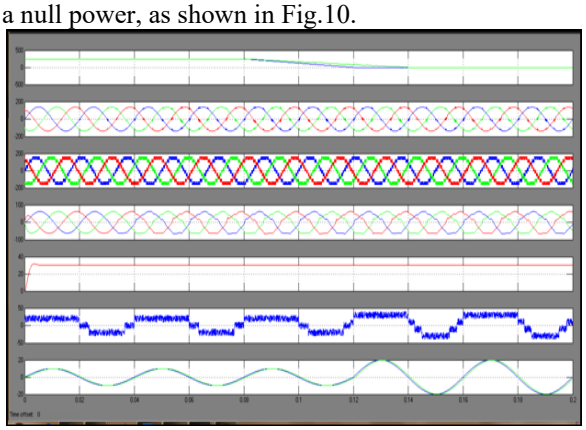

Fig.10. Simulation waveforms for a transient response of the active-power reference of u-phase battery module numbered 1 from 250 to 0 W when the active-power control for individual bridge cells was applied during charging operation.

This seamless operation is similar to that when a battery module becomes unavailable. Theoretically, any zero-sequence voltage with no restriction could be injected by the active power control of individual bridge cell. However, a limitation exists practically. Let r be defined as a ratio of the ac mains line-to-neutral peak voltage with respect to N times of the nominal battery module voltage in a cluster:

$$r = \sqrt{\frac{2}{3}}\frac{V_S}{NV_B} \quad (13)$$

As a grid-connected converter, the BESS has to produce an ac voltage higher than the ac mains voltage. The resulting voltage margin is used for zero-sequence voltage injection. Thus, the rms value V_{0max} can be given by

$$V_{o\,max} = \sqrt{\frac{3}{2}}NV_B - V_S[V] \quad (14)$$

The first term on the right-hand side of (14) refers to the maximum ac rms voltage produced by the BESS.

$$V_{0max} = \frac{1-r}{r}V_S[V] \quad (15)$$

Equation (15) implies that the BESS can produce three-phase currents with no distortion when the injected zero sequence voltage has an amplitude lower than $\sqrt{2}V_{0max}$

Fig.11 shows the relationship between the amplitude $\sqrt{2}V_0$ and the cascade count N when a failure of one, two or three battery modules occurs within one cluster. The curves show that, for the given number of faulty battery modules, the amplitude of $\sqrt{2}V_0$ decreases as N increases.

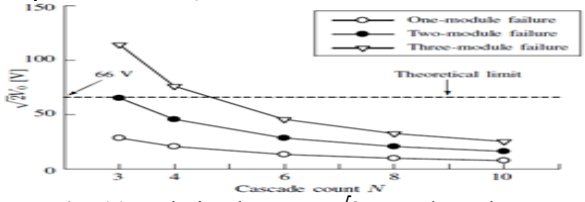

Fig. 11. Relation between $\sqrt{2}V_0$ and N when considering the failure of battery modules within a single cluster in the 140-V, 10-kW BESS.

TABLE IV

Comparison of Terminal Voltage of a Battery Module and Zero-Sequence Voltage for Different Cascaded Count N.

N	3	4	6	8	10
$V_B[V]$	5.18	37	25.9	18.5	14.8
$V_0[V]^{(1)}$	9.5	7.0	4.6 4.9[3]	3.5	2.7
$V_0[V]^{(2)}$	20.2	14.7	9.5 10.3[3]	7.0	5.6

(1) When p_{u1} reduces to half.
(2) When p_{u1} reduces to zero.
(3) These two values obtained from experiment

Table IV compares the nominal battery-module voltage V_B and the rms value V_0 for different values of N. The values of V_0 were calculated when p_{u1} is reduced to half of its original value and to zero, assuming that all of the bridge cells had the same power reference initially.

SIMULATION VERIFICATION OF ZVRT CAPABILITY

Verification procedure of ZVRT capability

Three single-phase controllable ac power supply units, each of which is rated at 200 V and 8 kW, were used to verify the ZVRT capability.

To verify the ZVRT capability, the BESS had voltage sags caused intentionally when the SOC-balancing control was performed. The SSBC-based BESS uses no additional technique except for the ones. This means that neither additional technique nor specific operation mode is required to provide ZVRT capability.

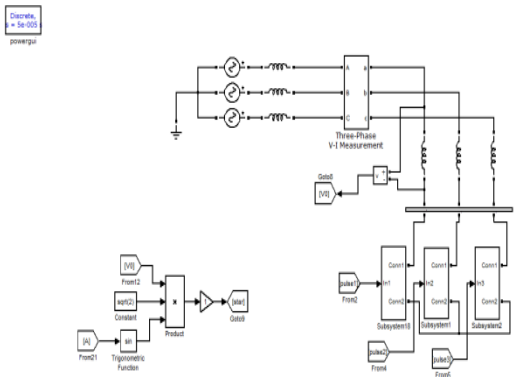

Fig.12. Simulation block diagram

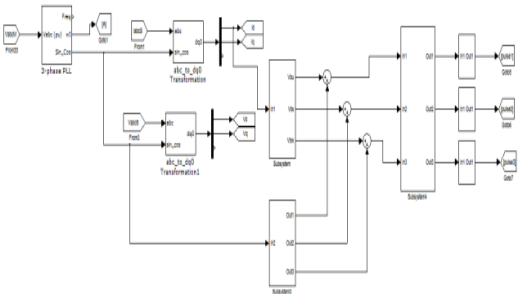

Fig.13. Control block diagram of simulation

Simulation Waveforms for ZVRT capability

Figs.14, 15 and 16 show simulation waveforms to verify ZVRT capability. Voltage sags occurred during the rated charging operation of 10 kW. Fig.14. shows the simulation waveforms when single-phase voltage sag with a depth of 100% occurred.

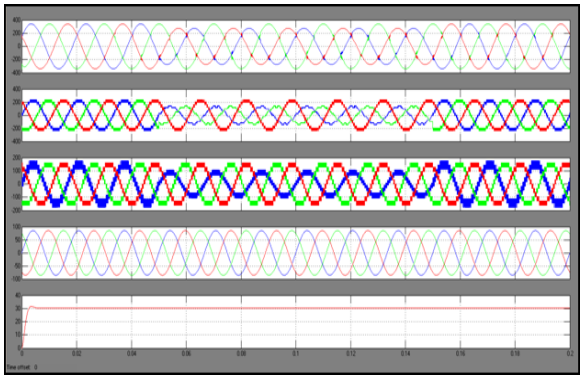

Fig.14. Simulation waveforms during the single-phase voltage sag with a depth of 100 % when using the SOC-balancing control during the rated charging operation of 10 kW.

The current THD on the u-phase cluster during the voltage sag was 2.3%. The three-phase cluster currents included neither distortion nor transient overshoot at the instant of the occurrence and restoration of the voltage sag.

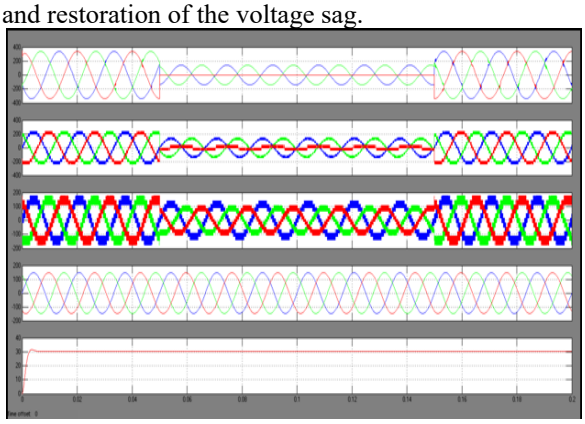

Fig.15. Simulation waveforms during the two-phase voltage sag with a depth of 100 % when using the SOC-balancing control during the rated charging operation of 10 kW.

Fig.15. shows the simulation waveforms when a two phase voltage sag with a depth of 100% occurred. No significant change was observed in the waveform of i_u, i_v and i_w as if no voltages sag occurred.

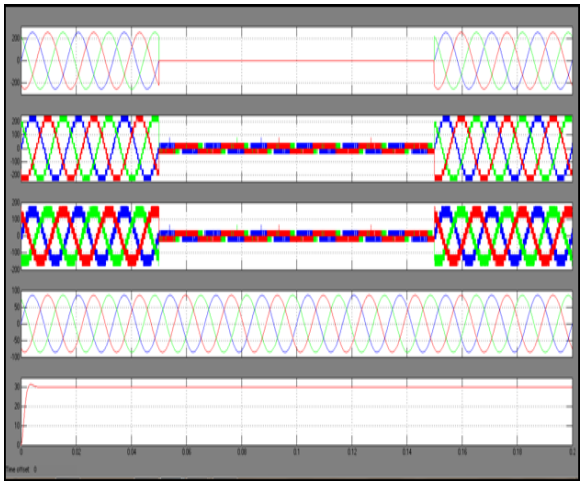

Fig.16. Simulation waveforms during the three-phase voltage sag with a depth of 100 % when using the SOC-balancing control during the rated charging operation of 10 kW

The three-phase currents slightly oscillated at the instant of the occurrence and restoration of the voltage sag. This low frequency oscillation resulted from a sudden reduction of the active power flowing from the power supply units.

CONCLUSION

This paper has presented a discussion on enhancement of performance, reliability, availability and flexibility of an SSBC-based BESS with fuzzy controller. Simulation results show the improvement of BESS with Fuzzy can provide the three phase balanced currents with reduced THD value compared to conventional system at various operating conditions. Estimating the active power of each bridge cell is simple and the accuracy has been verified by simulation results. Simulation waveforms have verified the ZVRT capability of the BESS under single phase, two-phase and three-phase voltage sags with a depth of 100%. The simulation results confirm the enhancement of performance, availability, and flexibility, because the BESS can maintain seamless and satisfactory operation on the most adverse conditions, such as battery modules failures or severe voltage sags occurrence.

REFERENCES

[1] L. H. Walker, “10-MW GTO converter for battery peaking service,” IEEE Trans. Ind. Appl., vol. 26, no. 1, pp. 63–72, Jan. 1990.

[2] R. Saupe, “The power conditioning system for the +/-8,5/17 MW energy storage plant of BEWAG,” in Conf. Proc. Third International Conference on Power Electronics and Variable-Speed Drives, Jul. 1988, pp. 218–220.

[3] T. Devries, J. Mcdowall, N. Umbricht, and G. Linhofer, "Cold storage," ABB Review, no. 1, pp. 38–43, 2004.
[4] J. Svensson, P. Jonest, and P. Halvarsson, "Improved power system stability and reliability using innovative energy storage technologies," in Conf. Proc. The 8th IEE International Conference on AC and DC Power Transmission, 2006. ACDC 2006. 2006, pp. 220–224.
[5] N. Wade, P. Taylor, P. Lang, and J. Svensson, "Energy storage for power flow management and voltage control on an 11-kV UK distribution network," in Conf. Proc. 20th International Conference and Exhibition on Electricity Distribution - Part 1, 2009. CIRED 2009, June 2009.
[6] H. Li, Y. Iijima, and N. Kawakami, "Development of power conditioning system (PCS) for battery energy storage systems," in Proc. Conf. 2013 IEEE ECCE Asia Downunder (ECCE Asia), June 2013, pp. 1295– 1299.
[7] N. Kawakami, Y. Iijima, H. Li, and S. Ota, "High efficiency power converters for battery energy storage systems," in The 2014 International Power Electronics Conference (IPEC-Hiroshima 2014 - ECCE-ASIA), May 2014, pp. 2095–2099.
[8] H. Akagi, "Classification, terminology, and application of the modular multilevel cascade converter (MMCC)," IEEE Trans. Power Electron., vol. 26, no. 11, pp. 3119 –3130, Nov. 2011.
[9] W. Kawamura, M. Hagiwara, and H. Akagi, "Control and experiment of a modular multilevel cascade converter based on triple-star bridge cells," IEEE Trans. Ind. Appl., vol. 50, no. 5, pp. 3536–3548, Sept 2014.
[10] L. Tolbert, F. Z. Peng, and T. Habetler, "Multilevel converters for large electric drives," IEEE Trans. Ind. Appl., vol. 35, no. 1, pp. 36–44, Jan. 1999.

BALLA SATYA DURGA PRASAD
Completed B.TECH in Electrical & Electronics Engineering in 2014 from Prasiddha College of Engineering & Technology Affiliated to JNTUK, KAKINADA and Pursuing M.Tech form Kakinada Institute of Technological Sciences Affiliated to JNTUK, KAKINADA, Andhra Pradesh, India. Area of interest includes High Voltage Engineering.
E-mail id: prasadpcet204@gmail.com

B BABY
Completed B.Tech in Electrical &Electronics Engineering in 2006 from Dr. V.R.K Women's College of Engineering and Technology Affiliated to JNTUH, Hyderabad and M.Tech in Electrical Power Systems in 2014 from Siddhartha Institute of Engineering and Technology Affiliated to JNTUH, Hyderabad. Working as Assistant Professor at Kakinada Institute of Technological Sciences, Kakinada, Andhra Pradesh, India. Area of interest includes Power Systems and Generation.
E-mail id: babybadugu@gmail.com